Chapter 3

Fast Mixing and Reaction Initiation Control of Single-enzyme Kinetics in Confined Volumes*

Abstract

A device with femtoliter-scale chambers and controlled reaction initiation was developed for single-molecule enzymology. Initially separated substrate and enzyme streams were rapidly mixed in a microfluidic device and encapsulated in an array of individual microreactors, allowing for enzyme kinetics to be monitored with millisecond dead times and single-molecule sensitivity. Because the arrays of chambers were fabricated by micromolding in polydimethylsiloxane, the chambers were monodisperse in size, and the chamber volume could be systematically controlled. Microreactors could be purged and replenished with fresh reactants for consecutive rounds of observation. Repeated experiments with statistically identical initial conditions could be performed rapidly, with zero cross talk among chambers in the array.

3.1 Introduction

Enzymatic reactions are ubiquitous in living systems and are involved in virtually every process related to physiological functioning of the cell. Such reactions usually take place in the ultrasmall volumes of cellular compartments, often with just a few copies of relevant molecules. In vitro

*This chapter is adapted with permission from S.-Y. Jung, Y. Liu, and C. P. Collier, *Langmuir*, 24:4439–4442, 2008.

experimental measurements can be used to simplify complex biological processes by isolating and then correlating the key biochemical factors involved. These measurements are typically performed under ideal conditions, such as in dilute homogeneous solution. However, the biochemical reaction steps that occur in vivo take place under highly nonideal, crowded, and confined conditions in the cell, which can significantly affect their thermodynamic and kinetic properties [99, 121]. To better understand how to infer in vivo dynamics from in vitro experimental measurements, we have fabricated femtoliter-scale biomimic compartments in microfluidics-based devices for capturing real-time single-molecule enzyme dynamics in confined spaces.

Several methods have been reported for interrogating chemical reactions with single-molecule sensitivity in ultrasmall containers such as micelles, vesicles [16, 63], oil-dispersed droplets, and nanoliter to femtoliter wells defined in various substrates such as silicon, polycarbonate [153], and polydimethylsiloxane (PDMS). Etched optical fibers [112, 113] and zero-mode waveguides [81] have also been employed as microreactors. These were typically used to characterize biochemical reaction kinetics at steady state. However, it is also important to have the ability to observe transient behavior of biochemical systems. A common technological challenge in terms of measuring transient dynamics for all these methods is achieving a well-defined zero of time for initiating the reaction in the confined space to monitor kinetics at early times. Ismagilov [130] and Cate [82] have demonstrated very rapid mixing in oil-dispersed aqueous plugs in microfluidic devices; however, the sizes of the plugs were defined by channel dimensions, typically in the tens to hundreds of micrometers range. To the best of our knowledge, single-molecule sensitivity has not yet been demonstrated in these devices.

We have developed a device with millisecond dead times to enable the observation of single-enzyme reactions at early stages as well as at steady state. The microfluidic device that we are reporting here completely mixes reactants (such as enzyme, substrate, and inert biological macromolecules as crowding agents) in about 100 ms and traps them in arrays of femtoliter-scale chambers defined at the interface of a glass coverslip and PDMS [116].

Effective mixing is the main obstacle in reducing the dead time in a microfluidic device. Fluid flows in microfluidics are characterized by low Reynolds number and high Péclet number due to the dimensions of microchannels and flow rates. Under these conditions, diffusive mixing is very slow

and ineffective. Much effort has been devoted to facilitate mixing in this regime [18, 127, 128, 146]. Recently, chaotic advection generated by staggered-herringbone structures in a microchannel [144, 145] was shown to accelerate the mixing of two otherwise colaminar streams. This makes it possible to initiate a reaction with a well-defined time zero and well-mixed initial conditions. Optical lithography was used to fabricate raised features 5 μm in diameter on a master silicon template, which formed cavities in PDMS by micromolding. Each 5 μm chamber had a volume of approximately 100 fL (4.4 μm diameter with 6.5 μm height), as inferred from scanning electron microscopy (SEM) images of the microchambers.

In the device, fluid flowed in an inlet channel which was in registry with the array. A control valve in a second PDMS layer fabricated using multilayer soft lithographic techniques [164] intersected the flow channel in the bottom layer and could be hydraulically actuated (within a few milliseconds) to seal off the flow channel, trapping the liquid in the ultrasmall chambers. The femtoliter chambers were positioned in the field of view of an inverted optical microscope, and fluorescent products from enzymatic reactions were detected using a CCD camera. The excitation source was a mercury–xenon lamp that was attenuated with neutral density filters and controlled by a fast electronic shutter.

3.2 Materials and Methods

Beta-Galactosidase (β-Gal) was purchased from Calbiochem (San Diego, CA), and resorufin-β-d-galacto-pyranoside (RGP) was obtained from Molecular Probes (Eugene, OR). Bovine serum albumin (BSA) and sulforhodamine 101 (Texas Red) was purchased from Aldrich (St. Louis, MO). All chemicals were used without further purification for making aqueous solutions with Millipore 18 MΩ water (Billerica, MA). SU8-2025 and its developer were produced by MicroChem (Newton, MA). SU8-2005 was made by diluting SU8-2025 with cyclopentanone (Sigma Aldrich, St. Louis, MO).

The microfluidic devices were fabricated using multilayer soft lithographic techniques [18] (see the supporting information for details). Solutions were introduced to the microfluidic device by a syringe pump (SP101i, World Precision Instruments, Sarasota, FL) through polystyrene tubing and 23-gauge stainless steel needles (Technical Innovations, Brazoria, TX). The control valve was filled

with 18 MΩ water and deflected downward by compressed air (20 psi) to close the channel and seal the chambers. For leaking and mixing tests, 1 μM Texas Red solution was used in one of the inlets. For enzymatic reactions, 50 μM of RGP solution was reacted with solutions containing 4.5–9 ng/mL β-Gal.

Fluorescence images were obtained on an inverted epifluorescence microscope (Eclipse TE300, Nikon, Melville, NY) equipped with a CCD camera (CoolSNAP-HQ, Roper Scientific, Tucson, AZ) using a 100× oil-immersion objective (NA 1.4). Metamorph software from Universal Imaging Corp. (Downingtown, PA) was used to capture and process images. Captured images were transferred to Adobe Photoshop for further processing. A 200 W mercury–xenon arc lamp (Ushio, Japan) acted as the light source for excitation, and appropriate filter sets (G-2E/C filter combination, Nikon, Melville, NY) were used for Texas Red and resorufin detection. Photobleaching of resorufin during experiments was minimized by utilizing neutral density filter sets (ND 8 and ND 4) and synchronizing the CCD with a Lambda SC smart shutter (Sutter, CA). Resorufin solutions of known concentration were injected into the device and trapped in 100 fL chambers. The fluorescence intensity integrated over the area of a selected chamber showed a linear relationship with the concentration of resorufin. This was used later to calculate the increase of resorufin concentration as a function of time due to enzymatic reactions in chambers of the same volume.

3.3 Results and Discussion

The overall scheme of microfluidic device is depicted in figure 3.1. Substrate and enzyme solutions were introduced from two different inlets and mixed thoroughly after passing through the herringbone mixer. The homogeneous reaction mixture was then trapped in individual microchambers as soon as hydraulic pressure was applied to the control valve to push the chamber layer to the bottom of the channel on the coverslip.

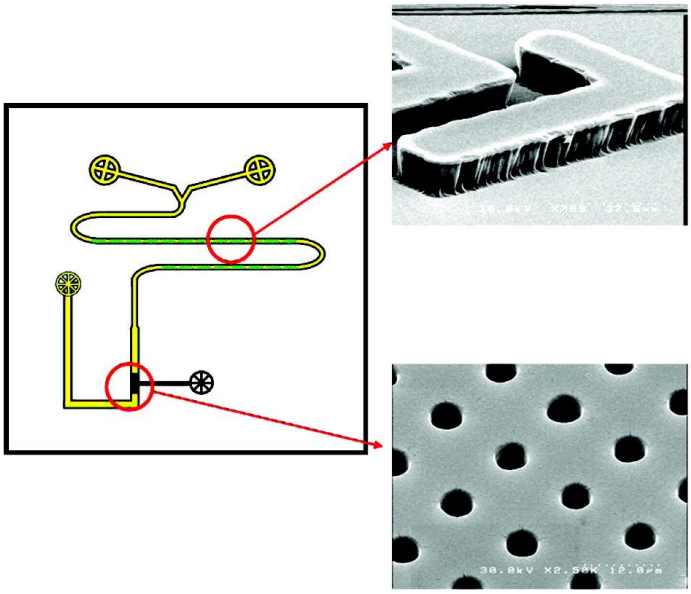

Figure 3.1. Layout of the microfluidic device including mixer, chamber array, and control valve. Inserts: SEM images of mixer mold (top), and array of chambers molded into PDMS (bottom).

3.3.1 Mixing and Encapsulation

Many control experiments to test the suitability of these devices for single-molecule enzymology were performed. The devices containing arrays of 100 femtoliter microchambers were tested with Texas Red solution in pH 7.4 buffer to show the thorough mixing by the chaotic mixer and the absence of leaking from or cross talk among the microchambers in the array. Figure 3.2 illustrates the effect of the chaotic mixer using fluorescence images of the main channel at different positions. Colaminar streams of 1 μM Texas Red solution and buffer-only solution were introduced at the two inlets by the syringe pump at a flow rate of 10 μL/min. The results of the mixing process can be visualized in the subsequent stages of the mixer; by the ninth stage, the flows appeared to be completely mixed. The fluorescence intensity of the homogeneous solution at this location corresponded to a calibrated resorufin concentration of 0.5 μM, which indicated complete mixing quantitatively. At the flow rates used, this occurred within about 140 ms, at which point the mixed flow could be trapped in the chambers by actuating the control valve. This short dead time ensured that early kinetics could be observed in this device.

PDMS is water permeable [124], so careful humidity control was necessary to minimize rapid

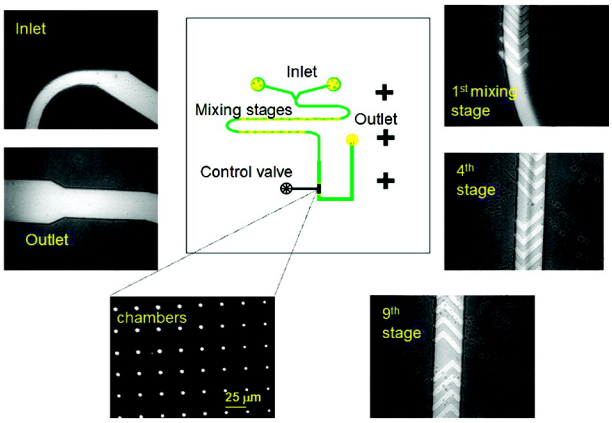

Figure 3.2. Mixing by chaotic advection by herringbone structures in the microfluidic channel. Fluorescence images show progress of mixing at different locations in the channel (arranged in clockwise order, starting with the inlet at the upper left).

evaporation of encapsulated solution in the femtoliter volumes of the chambers. To achieve this, the control valve reservoir located above the microchambers was filled with buffer solution. No sign of evaporation of the solutions in the microchambers was observed for as long as 30 min after the control valve was actuated. To test for cross talk between adjacent chambers due to leaking or diffusion of solute molecules through PDMS, a selected microchamber with Texas Red solution was photobleached by high-intensity light from the arc lamp through a closed iris. After the fluorescent dye in the selected chamber was bleached, recovery of fluorescence intensity was monitored for 20 min. Figure 3.3(d) shows line scans of fluorescence intensity from the chamber taken before (a), right after (b), and 20 min (c) after photobleaching. No fluorescence intensity increase could be observed from the bleached chamber, indicating an absence of cross talk between the selected chamber and its surrounding environment.

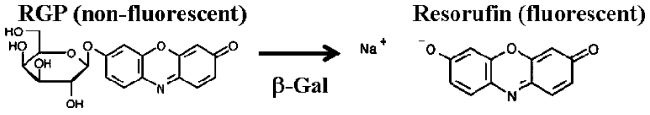

Scheme 3.1. Hydrolysis of RGP substrate by β-Gal to produce fluorescent resorufin.

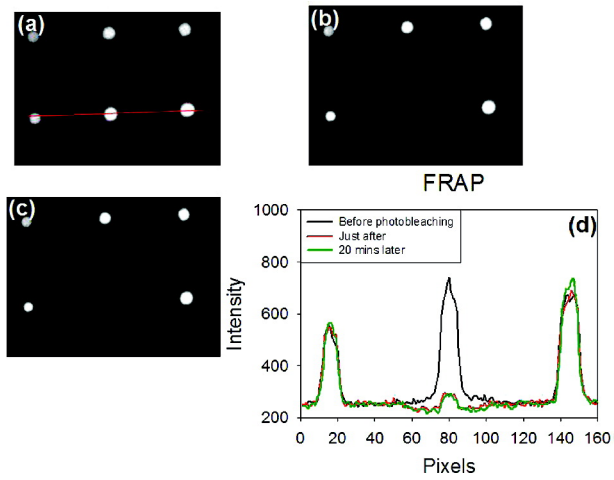

Figure 3.3. Line scans (d) of fluorescence intensity from images of an array of 100 fL chambers containing 0.5 µM Texas Red solution taken before (a), right after (b), and 20 min (c) after photobleaching the lower middle chamber through an iris.

3.3.2 Single-enzyme Experiments

After characterizing the basic properties of the device, enzymatic reactions in the microchambers were carried out as a proof of concept. β-Gal and RGP were used as the enzyme and substrate. Enzymatic cleavage of RGP by β-Gal releases fluorescent resorufin, with galactose as a by-product (Scheme 3.1). Enzymatic activity could be conveniently monitored by the increase of fluorescence intensity with time due to the accumulation of resorufin in the chambers (figure 3.4(a)).

A low concentration of β-Gal (4.5–9 ng/mL) was used such that on average, 0.5 to 1 enzyme would be trapped in each chamber. Figure 3.4(a) shows a typical snapshot of fluorescence intensity in six microchambers taken 60 s after the initiation of enzymatic reactions. After closing the control valve, a distribution of reaction rates was monitored by increasing fluorescence in the chambers. Figure 3.4(b) is a plot of mean product concentrations as functions of time, with associated linear regressions, showing discrete reaction rates corresponding to zero, one, or two enzymes per chamber. Observations of fluorescence intensity were recorded at 60 s intervals using a synchronized electronic shutter to prevent photobleaching and allow for a relatively long period of data acquisition (shutter open time was one second for each measurement). Error bars correspond to $\pm$ one standard deviation from the mean. The linear correlation coefficients for the fitted lines were 0.9946 (zero enzymes per

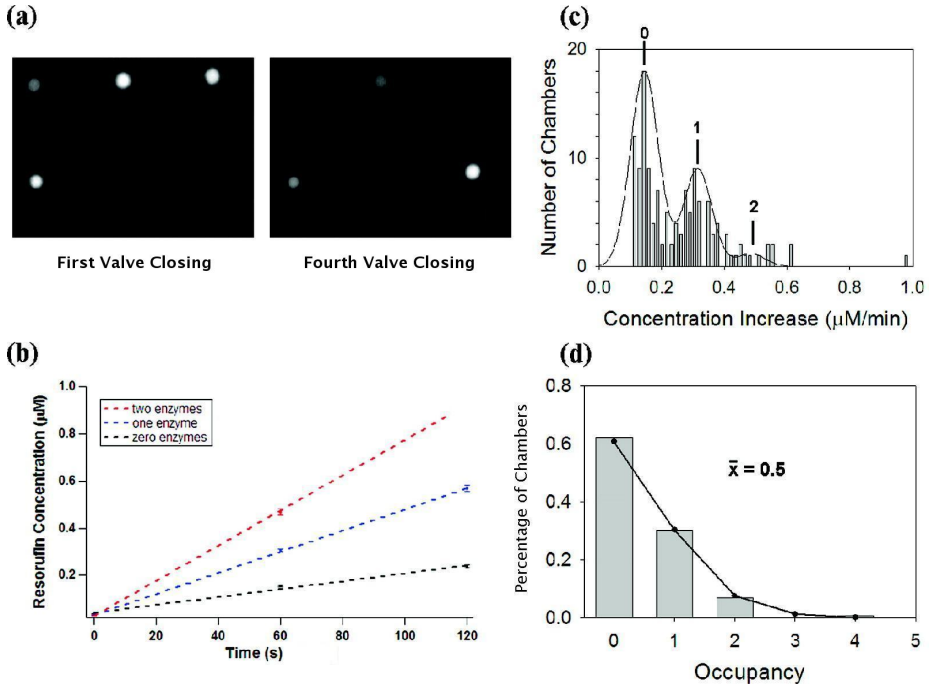

Figure 3.4. Enzyme reactions in microchambers. β-Gal concentration was 9 ng/mL (one enzyme per 100-femtoliter chamber on average) with 100 μM RGP for (a), and 4.5 ng/mL (0.5 enzymes per 100-femtoliter chamber on average) with 100 μM RGP for (b)–(d). Chambers were coated with 10 mg/mL BSA before experiments to minimize nonspecific binding of enzymes onto PDMS wall. (a) Fluorescence images of chambers taken 60 s after the initiation of enzymatic reactions. Subsequent opening and closing rounds of chambers by the control valve show no memory effect, which indicates negligible nonspecific adsorption of enzymes onto the chamber wall. (b) Mean product concentrations as functions of time, with associated linear fits, showing discrete reaction rates corresponding to zero, one, or two enzymes per chamber. Error bars correspond to ± one standard deviation from the mean. (c) The histogram of the fluorescence increase for 132 chambers was binned to groups corresponding to zero, one, or two enzymes in a chamber. (d) The percentage of chambers (bar) containing zero, one, or two enzymes agreed with a Poisson distribution (line) with a mean value of 0.5.

chamber), 0.9999 (one enzyme per chamber), and 0.9999 (two enzymes per chamber). The raw data from 395 independent measurements associated with this plot are included in the supporting information.

A histogram of the fluorescence increase for 132 chambers was binned to groups corresponding to zero, one, or two enzymes per chamber (figure 3.4(c)). The percentage of each group can be described

by a Poisson distribution with a mean value of 0.5 (figure 3.4(d)), as expected from the enzyme concentration employed. The initial rate of product molecule formation, 243 ± 30 resorufin per enzyme/s, was consistent with bulk stopped-flow and steady-state measurements (288 ± 33 resorufin per enzyme/s), performed by us (see the supporting information), and others [26]. When successive opening and closing rounds of the chambers were performed by actuating the control valve, the distributions changed, indicating that the enzymes were not surface bound, but free in solution. Importantly, the initial rate of reaction in different chambers remained roughly the same. This suggests that their catalytic activity was not affected by nonspecific adsorption to the chamber walls, which had been passivated with high concentrations of BSA (10 mg/mL) for 1 h before the measurements. This was corroborated by another control experiment where the enzymes were flushed out of the chambers, and then the solution containing only substrate but no enzymes was trapped. No fluorescence increase was detected over background levels due to weak autohydrolysis of the substrate.

Our device enables rapid gathering of kinetics data on the same chip, so it is especially useful for single-molecule studies where dynamic [88] or static [153] disorder must be thoroughly explored by analyzing a statistically significant ensemble of experiments. This can be achieved by flushing out the old reaction mixture from the chambers at the conclusion of a measurement with fresh, well-mixed solution of enzyme and substrate for 15 min. This flushing procedure resulted in no observed memory effects in reaction kinetics in the microchamber from one run to the next. Statistically independent reaction kinetics could be observed from the same chamber with each closing of the control valve.

3.4 Summary and Conclusions

A microfluidic platform combining rapid mixing and controlled reaction initiation in femtoliter-volume microreactors was developed and tested. As a proof of concept, single-enzyme reaction kinetics was measured with the device. Control experiments established the effective isolation of each microchamber from its neighbors in the array, without memory effects from previous experiments.

These devices enable access to early kinetics of single-molecule experiments, in addition to steady-state kinetics, made possible by a judicious combination of well-established microfluidic techniques.

It is straightforward to change the dimensions or contents of the chambers to mimic various features of real cellular compartments. For example, one could introduce inert crowding agents, such as BSA, to study the effect of molecular crowding on reaction kinetics [99]. To study the significance of geometric constraints [152], chambers of different shape, size, or topology may be fabricated in the same way. In particular, chambers smaller than 1 μm, from molds fabricated with electron-beam lithography, would provide spatial confinement on a scale matching confocal microscopy, without the need for surface chemistry to immobilize enzymes, which has been shown to affect reaction rates [100]. The microenvironment in a chamber could be further tuned in the time domain, through temporal control of solute concentration by adjustable osmosis between the aqueous compartments of the chamber and the control valve reservoir [124]. With the use of a passive chaotic mixer on chip, mixing is complete within 140 ms, which makes transient as well as steady-state behavior accessible for observation. This feature is especially suitable for biological studies where transient, nonequilibrium phenomena are ubiquitous. Furthermore, with the introduction of connecting channels among chambers, one would be able to study the diffusion-mediated coupling of individual reactors and accompanying emergent behavior such as spatial wave generation and pattern formation [14]. These devices represent the beginning of the fabrication of model systems that can be used to systematically track, in a general and quantitative way and with single-molecule sensitivity, the transitions in enzyme kinetics from ideal, in vitro experimental conditions toward the greater complexity found in living cells. Our system can be useful for other interesting questions as long as fluorescence can serve as a readout signal. For instance, the unfolding of single freely diffusing RNase H could be studied in our system to complement steady-state, spFRET measurements on surface immobilized enzymes [78] to reveal the early stages of protein conformational changes in confined biomimetic environments.

Each one of the chambers in the array was virtually identical in terms of size and shape, and may be thought of as an independent reactor. The number and density of chambers in an array can be increased significantly with submicrometer chambers fabricated with electron-beam lithography.

This will enable the acquisition of large numbers of measurements quickly, not only by observing many chambers in an array simultaneously, but by multiple repeated measurements on the same array (because the chambers can be flushed out and reused). This will allow a better statistical sampling of the distributions of kinetic behaviors in enzyme catalysis in confined and highly nonideal, but physiologically more realistic, nanoenvironments.

Acknowledgment

The authors thank Alireza Ghaffari at the Micro–Nano Fabrication Laboratory at Caltech for help with microfluidic device fabrication.

Supporting Information

Photolithography

PDMS molds were fabricated with multilayer photolithographic techniques. Briefly, negative tone photomasks for the control and mixer layers were printed on transparency films at 20,000 dots per inch resolution by CAD/Art Services (Bandon, OR). A chrome mask with arrays of 5 μm dots was purchased from MEMS and Nanotechnology Exchange (Reston, VA). To make the mold for the mixer–chamber layer, SU8-2005 was first spun at 2000 rpm on a piece of silicon wafer cleaned by 2-propanol. After soft baking (1 min at 65 ℃ and 2 min at 95 ℃), the 5 μm dot arrays as well as alignment marks were transferred from the chrome mask to the resist by UV exposure at 4.5 mW/cm^2 for 90 s, followed by post exposure baking (1 min at 65 ℃ and 1 min at 95 ℃), and development in SU8 developer. Patterns of 5 μm dots were further stabilized by hard baking at 150 ℃ for 5 min. Each 5 μm chamber had a volume of approximately 100 femtoliters (4.4 μm diameter with 6.5 μm height), as inferred from scanning electron microscopy (SEM) images of the microchambers. Another layer of 25 μm thick SU8-2025 photoresist was then spin coated on top of the dot pattern and soft baked (1 min at 65 ℃ and 3 min at 95 ℃). To align the staggered-herringbone mixer patterns relative to the array of dots, four corners of the silicon chip were carefully cleared with SU8 developer

to reveal the alignment marks on the mold. The mixer patterns were then transferred to the second resist layer through the transparency mask by UV exposure at 4.5 mW/cm^2 for 1 min. After post exposure baking (1 min at 65 ℃ and 3 min at 95 ℃) and development in SU8 developer, the patterns were hard baked at 150 ℃ for 5 min. The mold for the control layer was made separately in a similar manner using single-step photolithography. The main channel layer was also made using SU8-2025 photoresist. A piece of clean, dry # 1 coverglass (Fisher Scientific, Pittsburgh, PA) was coated with a uniform layer of 35 µm thick SU8-2025. After soft baking (1 min at 65 ℃ and 3 min at 95 ℃), the coated coverglass was exposed to UV illumination under the transparency mask for the channel layer at 4.5 mW/cm^2 for 1 min. Post exposure baking and development in SU8 developer revealed negatively defined channels in resist layer on the glass coverslip.

Multilayer Soft Lithography and Device Assembly

The final device consists of three layers: a main channel layer (bottom), an intermediate mixer–microchamber layer (middle) and a control layer (top). The top two layers were assembled using multilayer soft lithography [164]. Before application of the PDMS elastomer, all of the silicon molds were treated with chlorotrimethylsilane vapor for 5 min to prevent strong adhesion between the elastomer and photoresist after curing. The elastomer used in this experiment was RTV 615 from General Electric Silicones. A silicone elastomer mixture with excess polymer base (20:1 mass ratio of polymer base and curing agent) was spin coated onto the microchamber–mixer mold at 2400 rpm for 60 s and cured in an oven at 80 ℃ for 45 min. The control layer was prepared by pouring silicone elastomer with deficient polymer base (5:1 mass ratio of polymer base and curing agent) onto the control layer mold and baking at 80 ℃ for 45 min after the elastomer was degassed. The control layer was peeled from the mold and aligned with the PDMS coated microchamber–mixer mold. The two-layer PDMS assembly was then baked for two hours to bond the two layers together into a single structure which was then peeled from the microchamber–mixer mold. The gradient of curing agents at the interface of the two layers drives their migration from the top layer to the bottom, ensuring that the two layers are strongly bonded together by covalent cross-linking at the interface [164]. Finally, the bottom layer and top two layers were activated by oxygen plasma cleaning (plasma

cleaner PDC-32G, Harrick Scientific Corp., Ossining, NY) and bonded together by heat treatment in an oven at 80 ℃ overnight.

Stopped-flow Measurements

The kinetics of reference β-Gal–RGP reactions in bulk solution was monitored with a stopped-flow instrument (SX.18MV, Applied Photophysics, Surrey, UK). Final concentration of 0.19 nM β-Gal with 100 µM of RGP was mixed and the fluorescence increase due to the enzymatic generation of resorufin was measured. A typical plot of resorufin concentration increase as a function of time is shown in figure 3.5. The mean and standard deviation from five measurements gave the initial rate of resorufin formation as 288 $\pm$ 33 resorufin per enzyme/s, which is close to the rate from a single enzyme in a 100 fL chamber: 243 resorufin per enzyme/s.

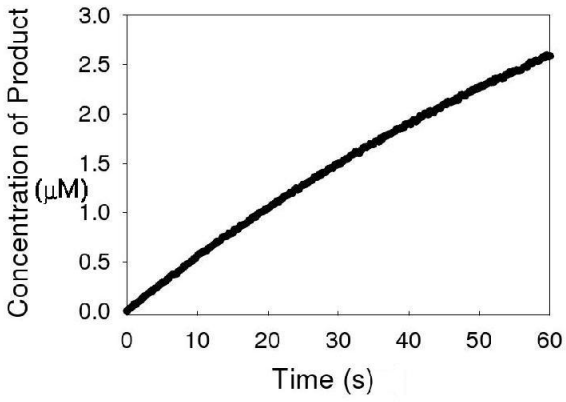

Figure 3.5. Bulk measurement of β-Gal enzyme activities by a stopped-flow instrument.